Massachusetts Institute of Technology

February 4th, 2013

Heterogeneity in the population response of a human cell line to hydrogen peroxide as measured by a genetically encoded sensor

Submitted by:

Sohail Feroz Ali

B.S., Chemical Engineering, Georgia Institute of Technology, 2007
M.S., Chemical Engineering Practice, Massachusetts Institute of Technology, 2012

Submitted to the Department of Chemical Engineering in partial fulfillment of the requirements for the degree of

Master of Science in Chemical Engineering

at the

MASSACHUSETTS INSTITUTE OF TECHNOLOGY

February 2013

Author Sohail Feroz Ali Digitally signed by Sohail Feroz Ali DN: c=US, st=Massachusetts, o=Massachusetts Institute of Technology, ou=Client CA v1, cn=Sohail Feroz Ali, email=sohail@MIT.EDU Date: 2013.02.04 22:45:35 +05'00'

Sohail Feroz Ali
Department of Chemical Engineering

Supervised by 2013.02.04 13:01:03 -05'00'

Hadley Sikes
Joseph R. Mares Assistant Professor of Chemical Engineering

Approved by

Patrick S. Doyle
Professor of Chemical Engineering
Chairman, Committee for Graduate Students

ABSTRACT

Genetically encoded ratiometric sensors can provide valuable mechanistic understanding of biological systems. Characterization of cellular response of these sensors is the first step in validating their use. Here, we characterize the response of a genetically encoded H_2O_2 sensor, HyPer, expressed in HeLa cells. Using quantitative fluorescence microscopy, we found significant heterogeneity in HyPer response among the cell population. Further analysis showed that the variation in HyPer response was dependent on expression of HyPer protein as well as on cell cycle phase. Cells with higher levels of expressed HyPer protein showed a stronger HyPer response to H_2O_2. Cells synchronized in S-phase showed a weaker HyPer response than unsynchronized cells. It was determined that this weaker response could be a function of higher antioxidant capacity in S-phase cells. The dependence of HyPer response on these factors needs to be accounted for to avoid experimental artifacts.

ACKNOWLEDGEMENTS

I am grateful to Professor Sikes for her constant support and guidance throughout my graduate work at MIT. I am also grateful to colleagues in Sikes lab that have helped with various aspects of this project, especially Brandon Heimer, Kara Huang, Kaja Kaastrup, and Joseph Lim. Adil Adatia , Abigail Klein and Michelle Tepelensky have made significant contributions to my work as UROPs. Dr. Fabienne Courtois from Trout lab has provided insightful advice on mammalian expression. Christopher Pirie from Wittrup lab taught me cell culture techniques and also gave HeLa cells as a gift. Also, Annie Gai from Wittrup lab provided valuable insights into transfection of mammalian cells.

Finally, I would like to thank my parents who have always supported me in all my endeavors with love and affection.

TABLE OF CONTENTS

INTRODUCTION 5

RESULTS 8

DISCUSSION 15

MATERIALS AND METHODS 17

LIST OF ABBREVIATIONS 19

SUPPLEMENTARY FIGURES 20

REFERENCES 22

INTRODUCTION

The discovery of free radicals in biological systems in the 1950s initiated extensive research efforts in deciphering their role in ageing and pathological processes (9). Initial research showed that reactive oxygen species (ROS) such as hydrogen peroxide (H_2O_2) were accidental byproducts of oxygen metabolism, and their existence was detrimental to cell survival (17). More recent investigations have revealed a significant role of ROS in maintenance of normal biological functions (11, 34, 39). Signaling molecules such as growth factors and cytokines stimulate cell growth and proliferation by producing low levels of ROS (4, 36). Moreover, macrophages and neutrophils employ a burst of ROS to kill pathogens (28). However, due to their high reactivity, higher than normal levels of ROS can cause irreversible damage to cellular organelles. Hence, cells have evolved regulatory mechanisms, such as antioxidant enzymes, to regulate intracellular ROS levels. An imbalance between ROS production and the antioxidant capacity leads to oxidative stress which has been implicated in ageing, cancer and neurodegenerative diseases.(1, 15). Although this dual nature of ROS in biology has been under extensive research, our understanding is predominantly qualitative in nature. Quantitative knowledge, such as concentration of ROS leading to a particular physiological affect, is very limited which precludes the development of mechanistic understanding of biological processes involving ROS.

Mechanistic knowledge of biological systems is critical for the efficient design of novel therapeutic strategies to address the wide variety of pathological conditions that have been linked to oxidative stress. Unraveling this information requires probes that can provide reliable detection while inducing minimal perturbations in the system. Recently, genetically encoded fluorescent proteins have been effectively employed as biosensors for reporting intracellular calcium, chloride, zinc and pH (5, 19, 29, 31, 38, 40). These non-invasive probes can give real-time spatial and temporal information and can be targeted to subcellular compartments. Furthermore, ratiometric variants of these probes can potentially provide reliable quantification that is independent of the number of fluorophores present in the system.

HyPer is a genetically encoded sensor that is sensitive to H_2O_2 (6, 24, 25). This probe consists of a circularly permuted yellow fluorescent protein inserted into the peroxide-sensing domain of the

bacterial transcription factor OxyR (2, 42). HyPer has two excitation peaks at 420nm and 500nm and an emission peak at 516nm. Upon stoichiometric reaction with H_2O_2, HyPer undergoes a reversible oxidation leading to a conformational change that causes changes in its spectral properties. The excitation peak at 420nm decreases whereas the excitation peak at 500nm increases which allows for a ratiometric readout that has been correlated with intracellular H_2O_2 present in the system (6, 24).

HyPer's remarkable specificity for H_2O_2, reversibility and low micromolar sensitivity to exogenously added H_2O_2 when expressed in cells makes it a good redox probe for tracking intracellular H_2O_2 concentration (24). Several studies have successfully used HyPer to track intracellular redox changes involved in cell signaling events (14, 21, 41). Furthermore, HyPer has been used in zebra fish to detect real-time H_2O_2 generation in wounds (10, 30) and in *C. Elegans* to monitor age-related increase in H_2O_2 levels (3).

Intracellular probes such as HyPer provide the possibility of robust quantification of ROS. Although HyPer has been used in diverse settings to track redox events, quantitative use of HyPer is still lacking. This requires a readout that is independent of number of fluorophores present in the system. The ratiometric readout provided by HyPer and other genetically encoded sensors, such as Pericam for calcium (29) and pHRed for pH (38), in principle can be independent of the number of fluorophores present, but this assumption has not always been rigorously validated. Frequently, literature studies report these sensors to be ratiometric due to the presence of dual excitation peaks which provides an internal self-calibration capability (6, 29, 38). However, the presence of the dual excitation peaks may not be a sufficient criterion for the sensor reading to be independent of the number of fluorophores present. A recent study showed that the ratio readout of a genetically encoded ratiometric zinc sensor was dependent on the sensor concentration at 'resting conditions'(31). Similarly, Sztretye et al., working with a ratiometric calcium sensor, reported slightly lower ratio values in intracellular regions of higher sensor expression, although this correlation was not seen across cells (37). Another study with a ratiometric chloride sensor reported the absence of a correlation between the sensor concentration and the calculated chloride concentration obtained from the ratiometric readout (40). The divergent observations reported by these studies indicate that assuming the ratiometric readout to be independent of sensor concentration based on the presence of dual excitation peaks

is not always sufficient. Dependence of ratio readout on sensor expression warrants a rigorous analysis at basal conditions and in response to stimulation to confidently validate the probe for a clear connection between ratiometric analysis and analyte concentration.

Furthermore, population-level quantitative understanding of biological processes is hindered by limitations of the measurement techniques as well as by the improper use of these methods. Spectroscopic methods, such as flow cytometry and spectrofluorimetry, provide population-level quantification of probe response (12, 18, 24); however, analysis of adherent cells with these methods requires trypsinization which can induce stress leading to artifactual generation of ROS in the system (16, 33). Besides spectroscopy, fluorescence microscopy is widely used for characterizing response of genetically encoded sensors. This method can potentially provide good quantification without the need of stress-inducing perturbations. However, quantitative use of fluorescence microscopy is very limited due to the small sample size (21, 24, 27). For example, Miller et al. analyzed 10-15 HyPer-expressing cells per experiment to detect intracellular H_2O_2 generation (26). A recent study with a HyPer derived pH sensor, SypHer, showed how quantitative results can be obtained using fluorescence microscopy provided a larger fraction of the population is analyzed (32).

Here, we use fluorescence microscopy to quantitatively characterize the response of HyPer in a population of adherent cells. Using image analysis, we were able to probe the HyPer response in a significantly larger fraction of cell population than in previous studies. This has revealed significant heterogeneity in HyPer response within the population. We have shed light on factors that affect HyPer response and that need to be accounted for so that the HyPer probe can be used more quantitatively.

RESULTS

Figure 1 shows the image processing steps that were used to quantify the response of HeLa cells stably expressing HyPer to stimulation with H_2O_2. HyPer images are obtained using 488/6nm and 415/30nm excitation filters before and after incubation with H_2O_2. Emission is collected at 525/40nm for both these channels. HyPer images are then corrected for uneven background illumination using the rolling ball algorithm in Image J (35). A radius of 200 pixels is used to eliminate background noise while minimizing loss of signal. Figure 1(C, D) shows how the algorithm reduces the background noise close to zero in both excitation channels.

The background corrected images are then used in the CellProfiler to identify HyPer expressing cells. The CellProfiler program scales the pixel intensities between 0 to 1 using the maximum image depth. Cell identification is done based on intensity thresholding using the Mixture of Gaussian (MoG) algorithm (8). This algorithm works by estimating Gaussian distributions to match the distribution of pixel intensities in the image. The identification process also uses the typical diameter of the objects (30-125μm) to exclude noise in the image. The cells identified are then filtered using eccentricity between 0-0.9. Once the regions are identified as HyPer expressing cells, HyPer ratio, (Emission at 488/6nm)/(Emission at 415/30nm), for each region is calculated by dividing the average pixel intensities for the region in the 488/6nm image by the average pixel intensity for the region in the 415/30nm image.

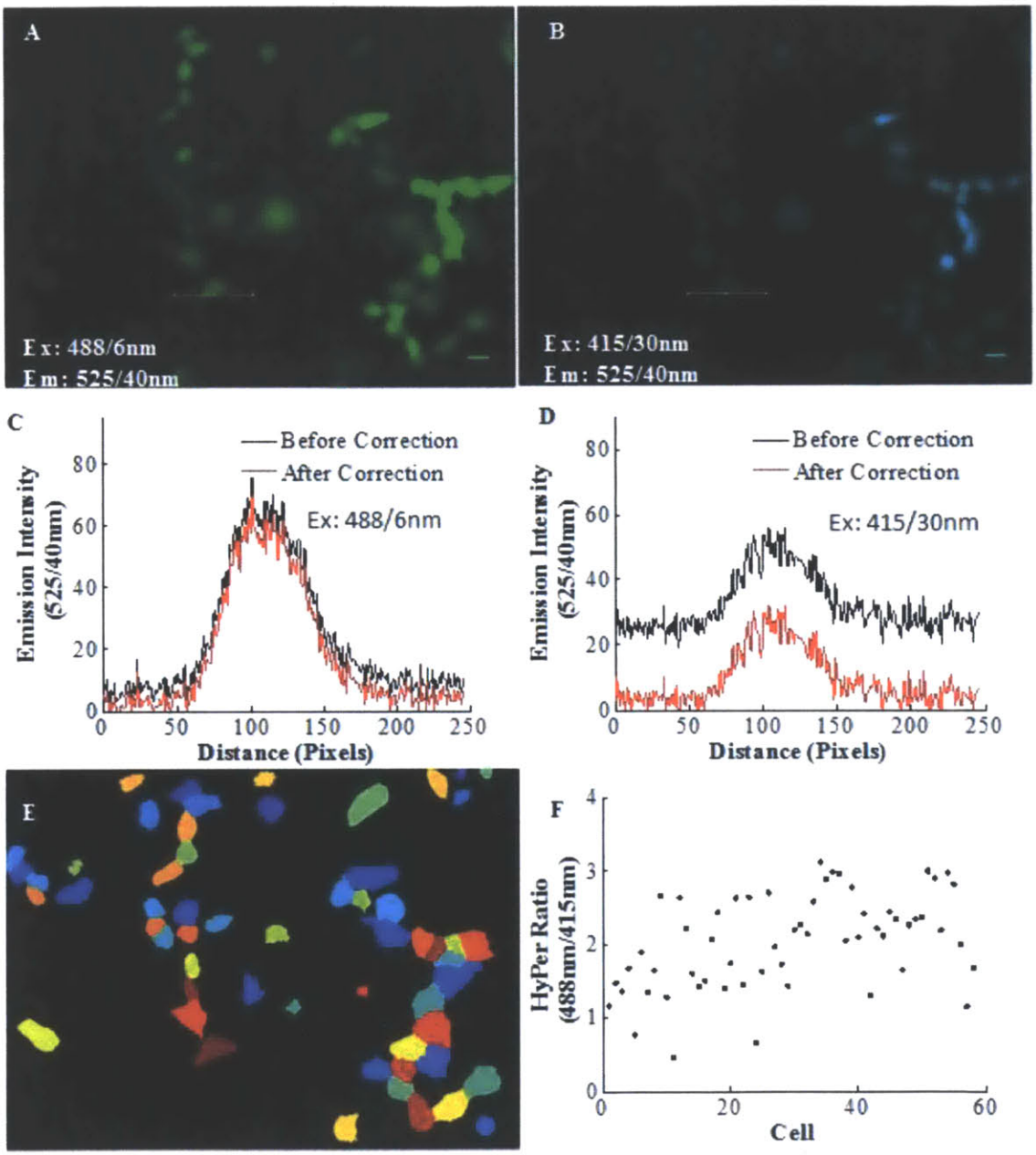

Figure 1: Images are processed before calculating the ratiometric HyPer readout. (A) Fluorescent image (488/6nm excitation, 525/40nm emission) of HeLa cells stably expressing the HyPer sensor protein under control of the CMV promoter. Scale bar: 25µm. (B) Fluorescent image of the same field of view (415/30nm excitation, 525/40 nm emission). Images shown in (A) and (B) were taken after a 10 minute incubation with 20 µM H_2O_2. (C, D) Intensity as a function of distance plots for the line shown in panels A and B before (black) and after (red) correction for background signal using the rolling ball algorithm (radius = 200 pixels) in Image J. (E) Cells expressing HyPer are identified in an automated fashion (CellProfiler) using the background-subtracted 488/6nm excitation image. (F) Calculated HyPer ratio for the cells identified in (E). The HyPer ratio is defined as the average emission intensity upon excitation with 488/6nm light divided by the average emission intensity upon excitation with 415/30nm light. Each data point represents the average HyPer ratio within one cell.

Figure 2 shows the HyPer ratio response to different concentrations of H_2O_2 in a population of adherent HyPer-HeLa cells. Below 5μM H_2O_2, the HyPer ratio remains close to its basal redox state. Above 10μM H_2O_2, the HyPer ratio changes showing the altered redox state due to the externally added H_2O_2. The HyPer signal saturates when treated with above 20μM H_2O_2. Furthermore, HyPer's response at 25μM and 50μM shows that the probe response is slightly muted compared to 20μM suggesting that HyPer might be undergoing over-oxidation that alters its response. Figure 2 strikingly shows that the HyPer response at a particular H_2O_2 concentration presents significant heterogeneity within the cell population. This cell-to-cell heterogeneity in HyPer's ratio is not apparent in the basal redox state.

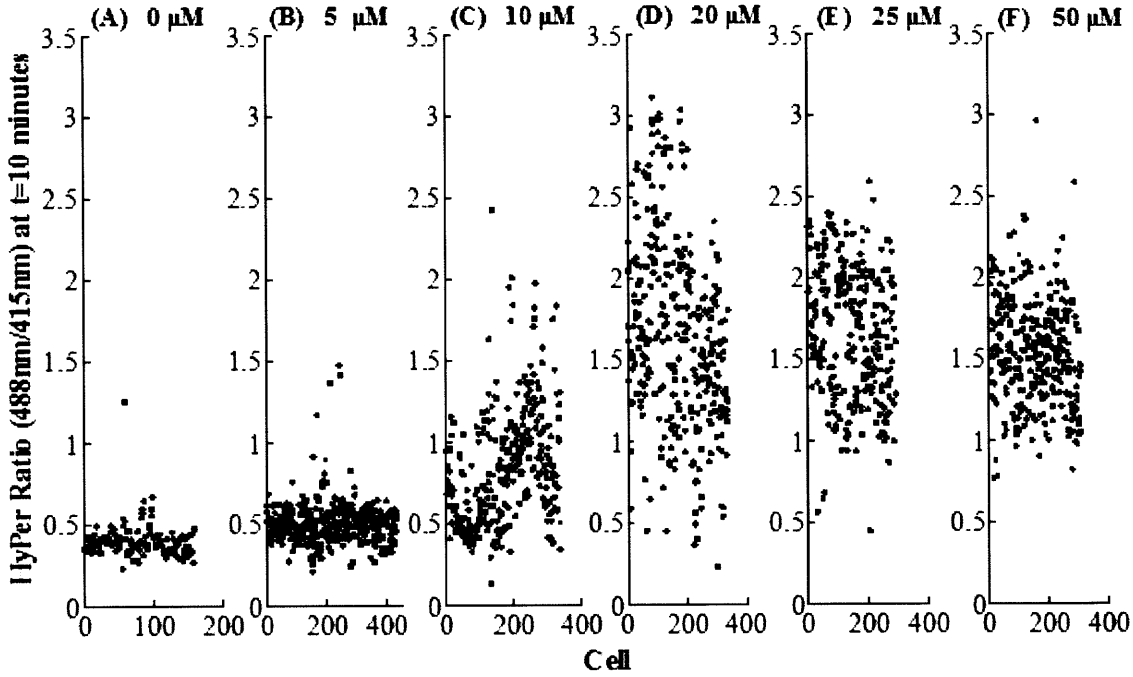

Figure 2: HyPer response to H_2O_2. HyPer-HeLa cells were incubated with 0-50μM H_2O_2 for 10 minutes. At the end of incubation, HyPer fluorescence images were obtained using 488/6nm and 415/30nm excitation filters. Emission was collected at 525/40nm. HyPer ratio was calculated from cell regions identified by CellProfiler using background corrected images. HyPer ratio for each region is shown for the indicated H_2O_2 concentrations 10 minutes after treatment. Each data point represents the HyPer ratio in one cell. (A) 0 μM (158 cells) (B) 5 μM (431 cells) (C) 10 μM (337 cells) (D) 20 μM (338 cells) (E) 25 μM (292 cells) (F) 50 μM (307 cells).

Dependence of HyPer response on expression level

Figure 3 shows that the HyPer ratio response to H_2O_2 stimulation depends on the expression level of the HyPer protein within a cell. Before addition of H_2O_2, the HyPer ratio is uniform across the cell population (Figure 3A). Furthermore, HyPer ratio does not show any dependence on expression level before H_2O_2 stimulation. We use the HyPer emission intensity at 488/6nm excitation wavelength as an indicator of expression level. The emission intensities at 488/6nm and 415/30nm excitation are linearly correlated (Figure 3B) which allows the use of either one as an indirect measure of expression. Using the emission intensity at 488/6nm excitation, Figure 3C shows that the basal HyPer ratio did not correlate with expression level. However, unlike the basal observation, the HyPer ratio 10 minutes after incubation with 20μM H_2O_2 is positively correlated to the HyPer expression level within that cell (Figure 3D). Higher expression seems to drive a higher HyPer ratio response. The Spearman correlation between the HyPer 488/6nm emission intensity at time zero and ratio response at 10 minutes was determined to be 0.70 ($p<0.05$) signifying a strong positive correlation. These results indicate that the expression level of HyPer within a cell influences the ratio response.

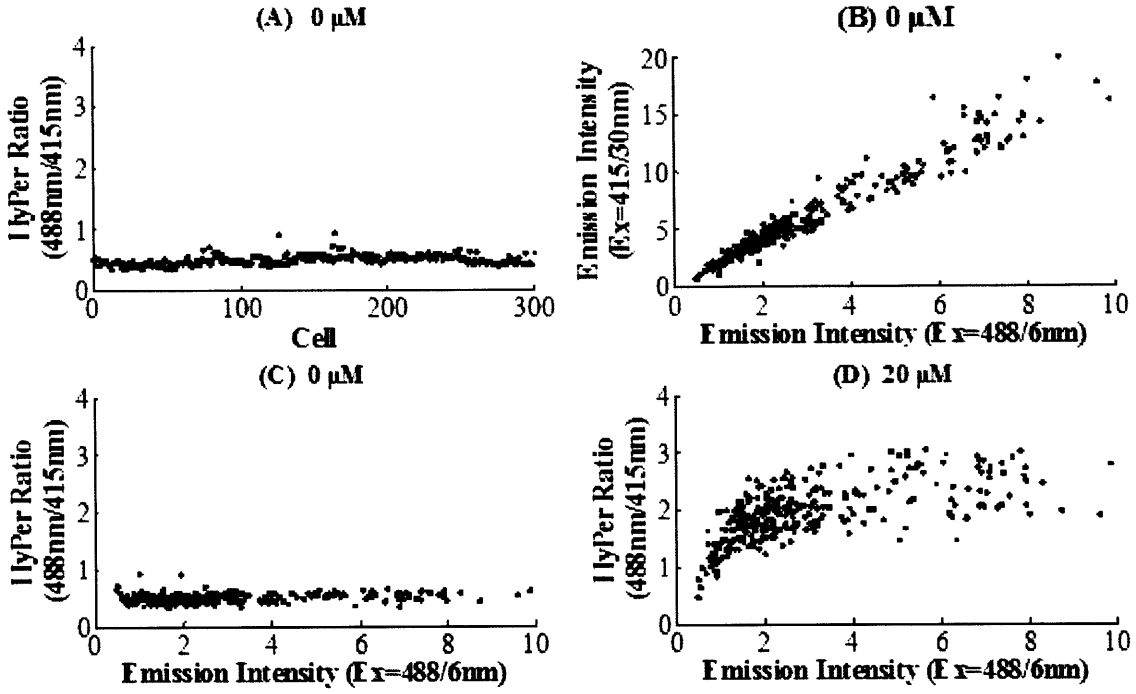

Figure 3: The HyPer ratio response to H_2O_2 correlates with the HyPer expression level. Images of HyPer-HeLa cells were obtained using 488/6nm and 415/30nm excitation filters before and after incubation with H_2O_2 for 10 minutes. Emission was collected at 525/40nm. HyPer ratio was calculated from cell regions identified by CellProfiler using background corrected 488/6nm excitation image. (A) HyPer ratio across cell regions before incubation with hydrogen peroxide. (B) Correlation between HyPer emission intensities when excited at 488/6nm and 415/30nm before addition of H_2O_2. (C & D) HyPer ratio as a function of emission intensity when excited with 488/6nm excitation filter, before (C) and after incubation with 20µM H_2O_2 for 10 minutes (D). All emission intensities reported here were scaled by a factor of 10^4.

Cell Cycle and HyPer Response

In addition to expression level, we studied the effect of cell cycle on HyPer ratio response. HyPer-HeLa cells were synchronized in G1/G0 phase using serum starvation and in S-phase using 2mM thymidine (7, 22). Figure 4 shows that there was no significant difference in HyPer response in G1/G0 synchronized cells; however, HyPer response in S-phase synchronized cells was significantly muted. This difference was further elaborated in the normal probability plot shown in Figure 5. For the S-phase synchronized cells, the probability of HyPer ratio within a certain cell being under 2.5 was 0.99 which was significantly less than the HyPer ratio observed in the G1/G0 synchronized cells as well as in the respective control groups.

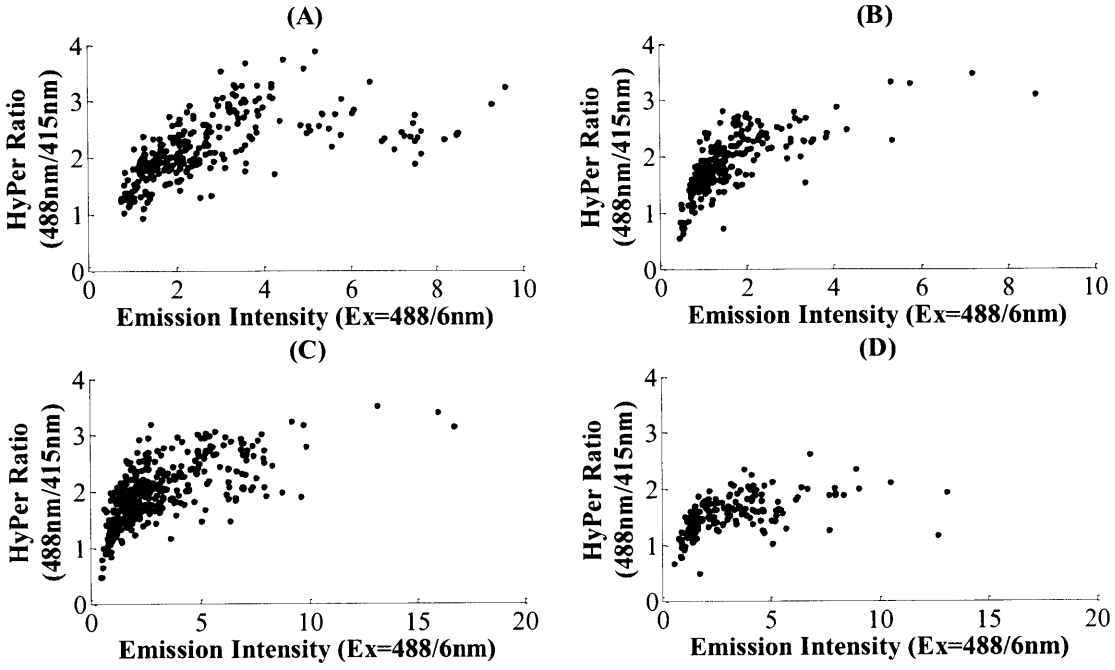

Figure 4: Cell cycle phase affects HyPer response. HyPer-HeLa cells were synchronized in G1/G0 phase using serum starvation or in S-phase using 2mM thymidine. Synchronized cells were treated with 20μM H_2O_2 for 10 minutes. Images of HyPer-HeLa cells were obtained using 488/6nm and 415/30nm excitation filters before and after incubation with H_2O_2 for 10 minutes. Emission was collected at 525/40nm. The HyPer ratio was calculated from cell regions identified by CellProfiler using background corrected 488/6nm excitation image. (A-B) The HyPer ratio response in cells cultured in full media (A) and cells cultured in serum free media (B). (C-D) The HyPer ratio response in cells cultured without thymidine (C) and cells cultured with 2mM thymidine (D). All emission intensities reported here were scaled by a factor of 10^4.

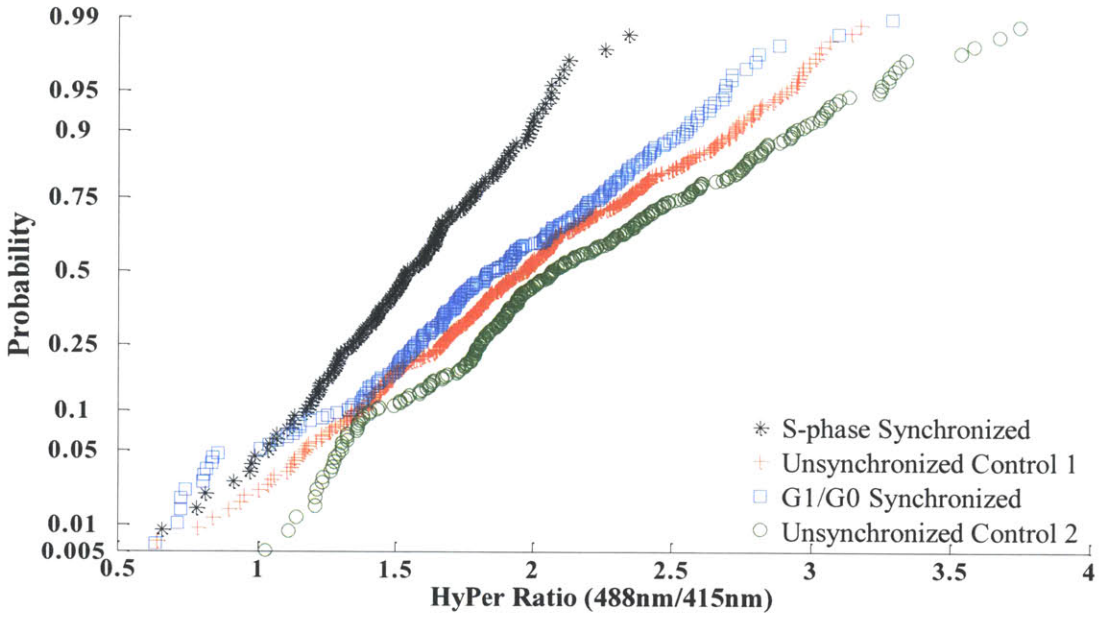

Figure 5: S-phase synchronized cells show muted HyPer response. Normal probability plot showing HyPer ratio response in synchronized cells. HyPer-HeLa cells were synchronized in G1/G0 phase using serum starvation or in S-phase using 2mM thymidine. Unsynchronized Control 1 and 2 served as control cell cultures for S-phase and G1/G0 phase synchronized cell cultures. Cells were treated with 20μM H_2O_2 for 10 minutes. Images of HyPer-HeLa cells were obtained using 488/6nm and 415/30nm excitation filters before and after incubation with H_2O_2 for 10 minutes. Emission was collected at 525/40nm. HyPer ratio was calculated from cell regions identified by CellProfiler using background corrected 488/6nm excitation image.

The muted HyPer response seen in S-phase synchronized cells can be due to an altered antioxidant capacity of the cells in S-phase. We investigated this by measuring the uptake of extracellularly added H_2O_2 in S-phase synchronized cells. After adding 20μM H_2O_2 in the extracellular medium, we followed the H_2O_2 concentration in the medium for 10 minutes (Supplementary Figure S1). HRP-ABTS assay was used to quantify the the extracellular H_2O_2 concentration at 2-minute intervals. We determined that the H_2O_2 decay rate constant was significantly higher in S-phase synchronized cells ($1.1 \times 10^{-3} \pm 0.2$ $min^{-1}cell^{-1}$) compared to unsynchronized cells ($6.6 \times 10^{-4} \pm 0.1$ $min^{-1}cell^{-1}$). This indicates that the antioxidant capacity in S-phase cells is significantly high. Since the timescale of HyPer response to H_2O_2 is significantly longer than the timescale of antioxidants reacting with H_2O_2 (11, 24), the higher antioxidant level in S-phase synchronized cells can potentially cause a lower HyPer ratio response as seen in Figure 4D.

DISCUSSION

Using quantitative fluorescence microscopy, we found significant cell-to-cell heterogeneity in the HyPer response to hydrogen peroxide in adherent HyPer-HeLa cells. Below a certain threshold (5μM H_2O_2), HyPer did not respond to extracellularly added H_2O_2. The dynamic range of HyPer was determined to be 5μM-20μM H_2O_2. Similar dynamic range was reported by Jiang et al. in HeLa cells (18). A slightly different dynamic range was reported in a study done in neurons, approximately 10μM-50μM H_2O_2 (13). This difference in dynamic range can be explained by variation in antioxidant capacity and cell membrane characteristics between cell lines. Furthermore, we saw that HyPer ratio response saturated over 20μM H_2O_2. HyPer also showed slightly muted response at concentrations higher than 20μM H_2O_2 suggesting that over-oxidation led to an altered response.

Our results show that the HyPer expression level within a cell leads to the cell-to-cell heterogeneity seen in HyPer response. Ratiometric variants of genetically encoded sensors, such as HyPer, are thought to provide a readout independent of the number of fluorophores present in the system, although this claim has not been rigorously tested at experimental conditions. At basal conditions, we found HyPer's response to be independent of its expression level within a cell. Similar observation was reported in studies done in *C. Elegans* expressing HyPer (3, 20). However, when we treated HyPer expressing cells with extracellularly added H_2O_2, we found that HyPer response correlated with HyPer expression within a cell. Image analysis showed that higher HyPer expression led to a higher HyPer ratio response when treated at a particular H_2O_2 concentration. This unexpected dependence of HyPer response on expression has not been reported in literature before. The HyPer ratio is derived from the changes in emission intensity at two excitations peaks (500nm and 420nm). The increase in HyPer ratio upon addition of H_2O_2 is due to increase in emission intensity at 500nm and decrease in emission intensity at 420nm. The increase in HyPer ratio with expression level seems to be driven by the decrease in emission intensity at 420nm. The decrease in 420nm emission on addition of H_2O_2 shows a positive correlation with HyPer expression level whereas the increase in 500nm emission does not show such a correlation (Supplementary Figure S2). This can cause the non-ratiometric rise in HyPer ratio as the number of fluorophores increase with higher expression level.

HyPer's response also showed dependence on cell cycle. HyPer-expressing cells synchronized in S-phase displayed a significantly muted response to H_2O_2 compared with unsynchronized cells. However, cells synchronized in G1/G0 phase behaved similar to unsynchronized cells. We determined that the S-phase synchronized cells had a significantly high antioxidant capacity. Since the rate of reaction of antioxidants with H_2O_2 is faster compared to rate of reaction of HyPer with H_2O_2 (11, 24), the high antioxidant capacity can potentially neutralize the H_2O_2, thereby reducing the HyPer response. Glutathione, an important player in cellular antioxidant system, is known to be at a higher concentration in S-phase cells compared to quiescent cells (23). It is possible that the muted HyPer response to H_2O_2 in S-phase synchronized cells was due to the presence of this high antioxidant capacity.

The cell-to-cell heterogeneity in HyPer response makes quantification of HyPer response in adherent cells non-trivial. Assaying a few cells for HyPer response for understanding biological processes can lead to incorrect inferences due to significant heterogeneity in response. Hence, use of HyPer in adherent cell analysis should be done while reducing the heterogeneity in HyPer response. Based on our findings, this heterogeneity can be reduced by controlling HyPer expression level within the cell. Besides experimental methods, statistical methods can be employed to select a population of cells that can potentially provide a quantitative HyPer response based on parameters such as expression level and cell cycle phase. Moreover, spectral properties of HyPer probe can be re-engineered to remove the dependence of the readout on changes in the emission intensity at 420nm excitation peak.

HyPer probe provides the potential to quantitatively understand the biological role of hydrogen peroxide. HyPer's specificity and low micromolar sensitivity to H_2O_2 allows reliable detection of intracellular redox processes. However, to appreciate the full capability of this probe, quantitative methods need to be employed to analyze HyPer's response in a significant fraction of the cell population. Moreover, the dependence of HyPer response on expression level and cell cycle phase needs to be accounted for to avoid experimental artifacts. This is critical for moving beyond qualitative findings and to obtain a true mechanistic understanding of ROS processes. Moreover, it is highly recommend that the ratiometric property of genetically encoded sensors should always be validated under experimental conditions of interest. This will ensure that the sensor can provide a ratiometric readout that is independent of the sensor concentration.

MATERIALS AND METHODS

Materials

EMEM and FBS were sourced from ATCC. Penicillin-streptomycin was from EMD Millipore. HyPer plasmid (pHyPer-cyto) was from Evrogen. Lipofectamine was from Life Technologies. PBS, thymidine and G418 were from Sigma-Aldrich. H_2O_2 was from BDH Chemicals. HRP and ABTS were from Alfa Aesar and Tokyo Chemicals, respectively.

Methods

Cell Culture and Transfection

HeLa cells were cultured in EMEM supplemented with 10% FBS and 1% penicillin-streptomycin. The cell cultures were maintained in a 37°C humidified incubator in the presence of 5% CO_2. Media was changed every 3 days and cells were passaged every 5-6 days.

HeLa cells were stably transfected with pHyPer-cyto vector containing the HyPer gene under CMV promoter. Cells were first transiently transfected with Lipofectamine following supplier's protocol. Twenty four hours after transfection, media was changed and supplemented with 700μg/mL of G418. After two weeks, stable clones were selected by picking fluorescent colonies using an Olympus widefield fluorescence camera (IX81). The selected colonies were expanded in medium containing 200μg/mL G418 in 96-well plates. The best fluorescing colony was kept for subsequent experiments. The stable cell HyPer-HeLa line was cultured in 200μg/mL G418 to maintain selection pressure and remove non-fluorescing cells.

For imaging, HyPer-HeLa cells were plated at a density of $2x10^4$ cells per well for approximately 42 hours in 96-well plate without G418. Before imaging, each well was washed with pre-warmed PBS (pH 7.4), and incubated with 150uL of 20uM H_2O_2 in PBS for 10 minutes at room temperature.

Cell Cycle Synchronization

For S-phase synchronization, HyPer-HeLa cells were grown as mentioned above in the presence of 2mM thymidine (7). Control cultures were grown similarly in absence of thymidine. For G1/G0 synchronization, cells were plated at a density of $1x10^4$ cells per well in EMEM with 10% FBS. After culturing for 24 hours, cells were washed with PBS (pH 7.4) and placed in

serum-free media for additional 24 hours before imaging (22). Control cultures were grown similarly except the replaced media contained 10% FBS.

Imaging

HyPer imaging was done using an Olympus widefield fluorescence microscope (IX81) and Prior Lumen2000 lamp. Images were acquired with a 20X Olympus objective. The 96-well plate was clamped on the stage to obtain same view-field images before and after the incubation with H_2O_2. HyPer fluorescence images were taken using Chroma D415/30x and Semrock FF01-488/6-25 excitation filters while emission was collected using a Semrock FF02-525/40-25 filter. Both images have 1600x1200 pixel density at 16-bit resolution. Exposure time was set at 300ms with the lamp intensity at 25%. Images were taken using a Retiga 2000R camera. The microscope, lamp and camera settings were kept constant throughout this study.

Image Analysis

HyPer images were background subtracted using the rolling ball algorithm (radius=200 pixels) in ImageJ (35). These images were then used to identify cell regions in CellProfiler software (8) based on intensity thresholding. The thresholding algorithm used was 'Mixture of Gaussian Adaptive.' The regions determined were filtered using a size criterion of 30-125 pixels and eccentricity of 0-0.9. HyPer ratio for a particular region was calculated as the average pixel intensity in HyPer-long channel divided by the average pixel intensity in HyPer-short channel in that region.

HRP-ABTS Assay

HyPer-HeLa cells, seeded at $1x10^6$ cells in $10cm^2$ dishes, were grown as mentioned above without G418 for 48 hours. Cells were then washed with PBS (pH 7.4) and incubated with 10mL of 20uM H_2O_2 in PBS (pH 7.4) for 10 minutes. 150µL samples were drawn every two minutes. These were treated with 50µL of 2.5mM ABTS and 10µl of 3mg/mL HRP. Absorbance was measured at 405nm using Tecan M200 plate reader in a 96-well plate.

LIST OF ABBREVIATIONS

ABTS- 2,2'-azino-bis(3-ethylbenzothiazoline-6-sulphonic acid)
EMEM- Eagle's Minimum Essential Medium
FBS- Fetal Bovine Serum
HRP- Horseradish Peroxidase
H_2O_2- Hydrogen Peroxide
PBS- Phosphate Buffered Saline
ROS- Reactive Oxygen Species

SUPPLEMENTARY FIGURES

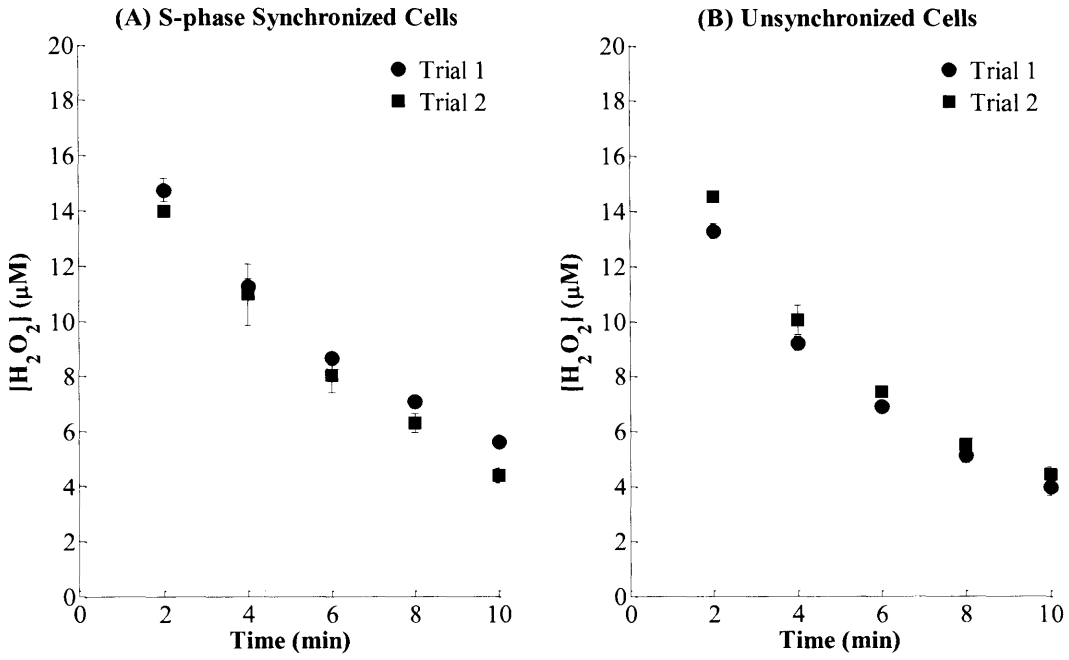

Figure S1: HRP-ABTS assay is used to measure antioxidant capacity by following the H_2O_2 decay kinetics in S-phase synchronized (A) and unsynchronized cells (B). 20μM H_2O_2 is added in the extracellular medium. Samples are withdrawn every 2 minutes to measure the remaining H_2O_2 concentration. Each data point is the average of three measurements. Error bars represent one standard deviation. The H_2O_2 decay constant calculated from the shown kinetic data is normalized by the number of cells present in the samples. Cells are counted from brightfield images obtained using a 20X magnification lens. Average cell count was 117±22 (n=4 images) in S-phase synchronzied sample and 227±24 (n=6 images) in unsynchronized sample.

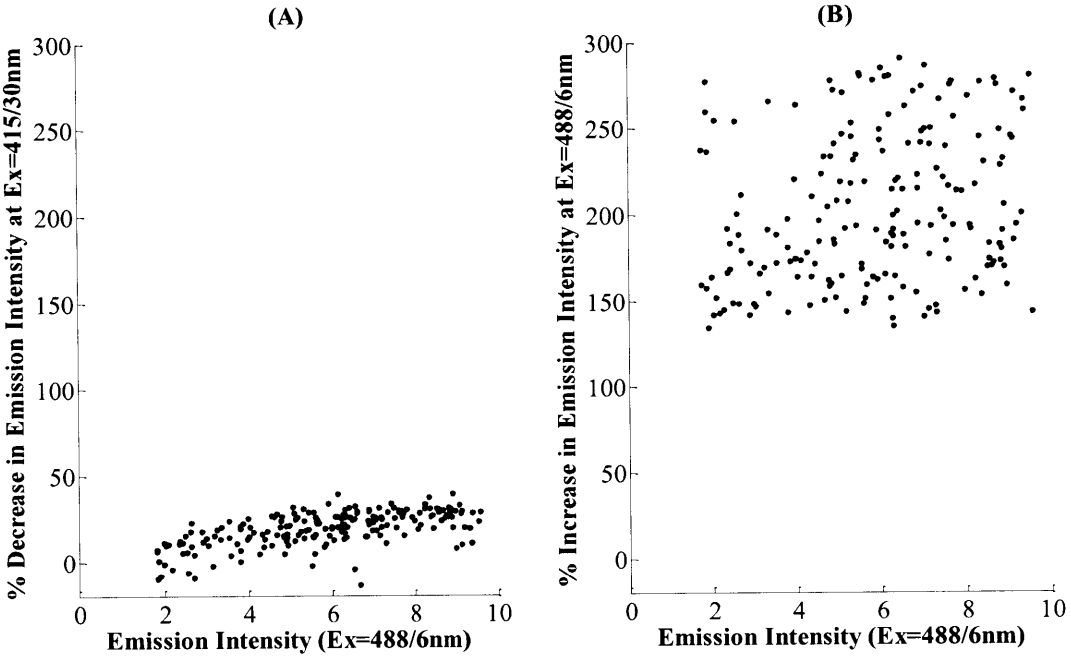

Figure S2: The percent decrease in emission intensity at 415/30nm excitation correlates with HyPer expression level. Images of HyPer-HeLa cells were obtained using 488/6nm (for 500nm excitation peak) and 415/30nm (for 488nm excitation peak) excitation filters after incubation with H_2O_2 for 10 minutes. Emission was collected at 525/40nm. HyPer ratio was calculated from cell regions identified by CellProfiler using background corrected 488/6nm excitation image. (A) Percent decrease in emission intensity at 415/30nm excitation 10 minutes after addition of H_2O_2 as a function of emission intensity at 488/6nm excitation (Spearman correlation=0.71). (B) Percent increase in emission intensity at 488/6nm excitation 10 minutes after addition of H_2O_2 as a function of emission intensity at 488/6nm excitation (Spearman correlation=0.16). Data points shown are within the 5-95% percentile. $p<0.01$ for Spearman correlation.

REFERENCES

1. Andersen JK. Oxidative stress in neurodegeneration: cause or consequence? Nat Med 10 Suppl: S18-25, 2004.

2. Aslund F, Zheng M, Beckwith J, and Storz G. Regulation of the OxyR transcription factor by hydrogen peroxide and the cellular thiol-disulfide status. Proc Natl Acad Sci U S A 96: 6161-6165, 1999.

3. Back P, De Vos WH, Depuydt GG, Matthijssens F, Vanfleteren JR, and Braeckman BP. Exploring real-time in vivo redox biology of developing and aging Caenorhabditis elegans. Free Radic Biol Med 52: 850-859, 2012.

4. Bae YS, Kang SW, Seo MS, Baines IC, Tekle E, Chock PB, et al. Epidermal growth factor (EGF)-induced generation of hydrogen peroxide. Role in EGF receptor-mediated tyrosine phosphorylation. J Biol Chem 272: 217-221, 1997.

5. Baird GS, Zacharias DA, and Tsien RY. Circular permutation and receptor insertion within green fluorescent proteins. Proc Natl Acad Sci U S A 96: 11241-11246, 1999.

6. Belousov VV, Fradkov AF, Lukyanov KA, Staroverov DB, Shakhbazov KS, Terskikh AV, et al. Genetically encoded fluorescent indicator for intracellular hydrogen peroxide. Nat Methods 3: 281-286, 2006.

7. Bootsma D, Vos O, and Budke L. Studies on synchronous division of tissue culture cells initiated by excess thymidine. Exp Cell Res 33: 301-&, 1964.

8. Carpenter AE, Jones TR, Lamprecht MR, Clarke C, Kang IH, Friman O, et al. CellProfiler: image analysis software for identifying and quantifying cell phenotypes. Genome Biol 7: R100, 2006.

9. Commoner B, Townsend J, and Pake GE. Free Radicals in Biological Materials. Nature 174: 689-691, 1954.

10. Deng Q, Harvie EA, and Huttenlocher A. Distinct signalling mechanisms mediate neutrophil attraction to bacterial infection and tissue injury. Cell Microbiol 14: 517-528, 2012.

11. Dickinson BC, and Chang CJ. Chemistry and biology of reactive oxygen species in signaling or stress responses. Nat Chem Biol 7: 504-511, 2011.

12. Elsner M, Gehrmann W, and Lenzen S. Peroxisome-generated hydrogen peroxide as important mediator of lipotoxicity in insulin-producing cells. Diabetes 60: 200-208, 2011.

13. Enyedi B, Varnai P, and Geiszt M. Redox state of the endoplasmic reticulum is controlled by Ero1L-alpha and intraluminal calcium. Antioxid Redox Signal 13: 721-729, 2010.

14. Espinosa A, Garcia A, Hartel S, Hidalgo C, and Jaimovich E. NADPH oxidase and hydrogen peroxide mediate insulin-induced calcium increase in skeletal muscle cells. J Biol Chem 284: 2568-2575, 2009.

15. Finkel T, Serrano M, and Blasco MA. The common biology of cancer and ageing. Nature 448: 767-774, 2007.

16. Halliwell B. Oxidative stress in cell culture: an under-appreciated problem? Febs Lett 540: 3-6, 2003.

17. Harman D. The Aging Process. P Natl Acad Sci-Biol 78: 7124-7128, 1981.

18. Jiang J, Maeda A, Ji J, Baty CJ, Watkins SC, Greenberger JS, et al. Are mitochondrial reactive oxygen species required for autophagy? Biochem Biophys Res Commun 412: 55-60, 2011.

19. Kneen M, Farinas J, Li Y, and Verkman AS. Green fluorescent protein as a noninvasive intracellular pH indicator. Biophys J 74: 1591-1599, 1998.

20. Knoefler D, Thamsen M, Koniczek M, Niemuth NJ, Diederich AK, and Jakob U. Quantitative in vivo redox sensors uncover oxidative stress as an early event in life. Mol Cell 47: 767-776, 2012.

21. Kratschmar DV, Calabrese D, Walsh J, Lister A, Birk J, Appenzeller-Herzog C, et al. Suppression of the Nrf2-dependent antioxidant response by glucocorticoids and 11beta-HSD1-mediated glucocorticoid activation in hepatic cells. Plos One 7: e36774, 2012.

22. Lafontaine J, Tchakarska G, Rodier F, and Mes-Masson AM. Necdin modulates proliferative cell survival of human cells in response to radiation-induced genotoxic stress. Bmc Cancer 12: 234, 2012.

23. Li N, and Oberley TD. Modulation of antioxidant enzymes, reactive oxygen species, and glutathione levels in manganese superoxide dismutase-overexpressing NIH/3T3 fibroblasts during the cell cycle. J Cell Physiol 177: 148-160, 1998.

24. Malinouski M, Zhou Y, Belousov VV, Hatfield DL, and Gladyshev VN. Hydrogen peroxide probes directed to different cellular compartments. Plos One 6: e14564, 2011.

25. Markvicheva KN, Bilan DS, Mishina NM, Gorokhovatsky AY, Vinokurov LM, Lukyanov S, et al. A genetically encoded sensor for H2O2 with expanded dynamic range. Bioorg Med Chem 19: 1079-1084, 2011.

26. Miller EW, Taulet N, Onak CS, New EJ, Lanselle JK, Smelick GS, et al. Light-Activated Regulation of Cofilin Dynamics Using a Photocaged Hydrogen Peroxide Generator. J Am Chem Soc, 2010.

27. Mishina NM, Tyurin-Kuzmin PA, Markvicheva KN, Vorotnikov AV, Tkachuk VA, Laketa V, et al. Does cellular hydrogen peroxide diffuse or act locally? Antioxid Redox Signal 14: 1-7, 2011.

28. Murray PJ, and Wynn TA. Protective and pathogenic functions of macrophage subsets. Nat Rev Immunol 11: 723-737, 2011.

29. Nagai T, Sawano A, Park ES, and Miyawaki A. Circularly permuted green fluorescent proteins engineered to sense Ca2+. Proc Natl Acad Sci U S A 98: 3197-3202, 2001.

30. Niethammer P, Grabher C, Look AT, and Mitchison TJ. A tissue-scale gradient of hydrogen peroxide mediates rapid wound detection in zebrafish. Nature 459: 996-999, 2009.

31. Park JG, Qin Y, Galati DF, and Palmer AE. New sensors for quantitative measurement of mitochondrial Zn(2+). Acs Chem Biol 7: 1636-1640, 2012.

32. Poburko D, Santo-Domingo J, and Demaurex N. Dynamic regulation of the mitochondrial proton gradient during cytosolic calcium elevations. J Biol Chem 286: 11672-11684, 2011.

33. Reiners JJ, Jr., Mathieu P, Okafor C, Putt DA, and Lash LH. Depletion of cellular glutathione by conditions used for the passaging of adherent cultured cells. Toxicol Lett 115: 153-163, 2000.

34. Rhee SG. Cell signaling. H2O2, a necessary evil for cell signaling. Science 312: 1882-1883, 2006.

35. Schneider CA, Rasband WS, and Eliceiri KW. NIH Image to ImageJ: 25 years of image analysis. Nat Methods 9: 671-675, 2012.

36. Sundaresan M, Yu ZX, Ferrans VJ, Irani K, and Finkel T. Requirement for generation of H2O2 for platelet-derived growth-factor signal-transduction. Science 270: 296-299, 1995.

37. Sztretye M, Yi J, Figueroa L, Zhou J, Royer L, and Rios E. D4cpv-calsequestrin: a sensitive ratiometric biosensor accurately targeted to the calcium store of skeletal muscle. J Gen Physiol 138: 211-229, 2011.

38. Tantama M, Hung YP, and Yellen G. Imaging intracellular pH in live cells with a genetically encoded red fluorescent protein sensor. J Am Chem Soc 133: 10034-10037, 2011.

39. Veal EA, Day AM, and Morgan BA. Hydrogen peroxide sensing and signaling. Mol Cell 26: 1-14, 2007.

40. Waseem T, Mukhtarov M, Buldakova S, Medina I, and Bregestovski P. Genetically encoded Cl-Sensor as a tool for monitoring of Cl-dependent processes in small neuronal compartments. J Neurosci Methods 193: 14-23, 2010.

41. Weyemi U, Lagente-Chevallier O, Boufraqech M, Prenois F, Courtin F, Caillou B, et al. ROS-generating NADPH oxidase NOX4 is a critical mediator in oncogenic H-Ras-induced DNA damage and subsequent senescence. Oncogene 31: 1117-1129, 2012.

42. Zheng M, Aslund F, and Storz G. Activation of the OxyR transcription factor by reversible disulfide bond formation. Science 279: 1718-1721, 1998.